

Axial-channeling radiation of MeV electrons in high-Z materials

Y. H. Ohtsuki

Department of Physics, Waseda University, Ohkubo 3, Shinjuku-ku, Tokyo 160, Japan

Y. Yamamura

Okayama College of Science, Ridai-cho, Okayama 700, Japan

M. Yoshimatsu

Rigaku Corporation, Matsubara 3-9-12, Akishima, Tokyo, Japan

(Received 13 January 1983)

Within the framework of classical mechanics, the radiation emitted by axially-channeled electrons in high-Z materials has been studied by computer simulations. The axial and temperature dependences of the axial-channeling radiation emitted by 5-MeV electrons have been investigated in detail for a Mo crystal. The intensity of the axial-channeling radiation emitted by 5-MeV electrons is compared with the forward-directed bremsstrahlung, which is also calculated numerically by computer simulation. We show that the intensity is much higher ($\sim 10^2$) than the intensity of the intense x-ray tube RU-1500.

I. INTRODUCTION

Several years ago, Vorobiev *et al.*¹ and Kumakhov² pointed out the possibility of spontaneous emission of γ quanta by relativistic channeling electrons, which was predicted to arise from transitions between the bound states formed in the field of atomic rows and planes. Kumakhov also predicted that the radiation power near maximum is higher by approximately 2 orders of magnitude than that of ordinary bremsstrahlung.

Recently, this new physical effect was first observed by Alguard *et al.*³ They observed the channeling radiation of 56- and 28-MeV positrons along the major planes and the major axes of a 18- μm -thick silicon crystal. Subsequently, many authors have successfully observed the photon spectrum emitted by the channeling of electrons and positrons.⁴⁻⁶

As for the low-energy electrons in relatively low-Z materials, Andersen *et al.*^{6,7} have theoretically and experimentally investigated the axial-channeling radiation in a silicon crystal for 3.5- and 4-MeV electrons, while Komaki *et al.*⁸ have calculated the photon energies and intensities of channeling radiation from the axially-channeled electrons in silicon and germanium single crystals, using the tight-binding approximation and the muffin-tin potential.

As was already pointed out by Kumakhov,^{2,9} the photon intensity of axial-channeling radiation of electrons is proportional to Z^2 (Z indicates the atomic number of the target atom), and the spectral density of the channeling radiation begins to exceed that of the ordinary bremsstrahlung at an electron energy of several MeV, at which intense x-ray will be emitted.

In this paper, we have calculated the photon intensity of axially channeled electrons in Mo and W crystals, using the classical binary-collision approximation¹⁰ and classical

electrodynamics.^{11,12} The photon intensity of channeling radiation was calculated by Fourier transform of an electron trajectory determined by the binary-collision approximation. In the case of high-Z materials, even if an electron energy is of order of several MeV, the number of bound levels is large enough to justify the use of classical mechanics to calculate the photon intensity emitted by axially channeled electrons.

II. COMPUTATION MODEL

The criterion governing the applicability of the classical description of electron channeling is that the number of quantum states be significantly larger than unity. For axial channeling of electrons, the number of states is given approximately by¹³

$$n_a = \gamma Z^{1/3} \frac{4a_0}{d}, \quad (1)$$

where a_0 is the Bohr radius, d is the distance between the string atoms, and $\gamma = (1 - v^2/c^2)^{-1/2}$ is the relativistic factor. As is seen from this formula, the number of levels increases with rising energy.

For the case of planar channeling of electrons, the number of states is given by

$$n_p = \gamma^{1/2} 4a_0 (Nd_p)^{1/2}, \quad (2)$$

where N is the atomic number density, and d_p is the interplanar distance.

Tables I and II give the values of n_a and n_p for various energies, targets, and channels of present interest. The critical angles are also listed for later discussions. These tables tell us that the axial case is "more classical" than the planar case and that axial channeling in high-Z materials such as Mo and W crystals can be reasonably treated within the framework of classical mechanics.

TABLE I. Number of levels and critical angles for electron planar channeling.

Target	Energy (MeV)	γ	Direction	Critical angle	Number of levels n_p
Mo	4	8.8	(100)	0.20	2.0
	5	10.7	(100)	0.19	2.2
Mo	4	8.8	(110)	0.24	2.4
	5	10.7	(110)	0.22	2.6
Mo	4	8.8	(111)	0.15	1.5
	5	10.7	(111)	0.14	1.7
W	4	8.8	(111)	0.18	1.5
	5	10.7	(111)	0.17	1.7

In the present simulation, an electron trajectory in a channel is described as a sequence of straight lines between collisions of an electron with the atoms in the string. Details of the simulation procedure have been described in Refs. 10 and 12. As the attractive potential between an electron and an atom in the string, the Moliere approximation to the Thomas-Fermi (TF) potential was employed. The effect of thermal vibration is also taken into account in a usual manner.¹⁰

The energy radiated by an electron per unit frequency and per unit solid angle is given in classical electrodynamics by the formula¹¹

$$\frac{d^2E}{d\omega d\Omega} = 2 |\vec{A}(\omega)|^2, \quad (3)$$

where $\vec{A}(\omega)$ is a vector proportional to the Fourier components of the electric field intensity,

$$\vec{A}(\omega) = \left[\frac{e^2}{8\pi^2 c} \right]^{1/2} \int_{-\infty}^{\infty} dt \exp \left[i\omega \left(t - \frac{\vec{n} \cdot \vec{r}(t)}{c} \right) \right] \times \frac{\vec{n} \times [(\vec{n} - \vec{\beta}) \times \dot{\vec{\beta}}]}{(1 - \vec{n} \cdot \vec{\beta})^2}. \quad (4)$$

\vec{n} is a unit vector in the direction of the emitted γ photon, $\vec{\beta} = \vec{v}/c$, \vec{v} being the velocity, and $\vec{r}(t)$ is specified by the electron trajectory. Once $\vec{r}(t)$ is specified for the entrance condition, the vectors $\vec{\beta}$ and $\dot{\vec{\beta}}$ can be determined.

III. AXIAL-CHANNELING RADIATION OF ELECTRONS IN CRYSTALS

The classical treatment of positron and electron channeling is similar to the channeling theory of light ions.

Neglecting multiple scattering and energy-loss effects the transverse energy E_{\perp} for motion perpendicular to the considered channel axis is conserved, i.e.,

$$E_{\perp} = \frac{p_r^2}{2m\gamma} + \frac{L^2}{2m\gamma r^2} + U(r), \quad (5)$$

where p_r is the radial momentum component, L the angular momentum, and r the distance between the electron and the atomic string. $U(r)$ is the string potential for the axial channeling, and the following Lindhard's standard potential¹⁴ is often used:

$$U(r) = -\frac{Ze^2}{d} \ln \left[\frac{3a_{\text{TF}}^2}{r^2} + 1 \right]. \quad (6)$$

The last two terms in Eq. (5) form an effective potential,

$$W(r, L) = \frac{L^2}{2m\gamma r^2} + U(r). \quad (7)$$

If one neglects the effects of thermal vibration, both the transverse energy and the angular momentum are constants of motion, and they are determined by the entrance condition at the crystal surface. Since the r dependence of $U(r)$ is weaker than r^{-2} at small distance, the effective potential has a local minimum for $L > 0$. This means that the electron trajectories are spirals around the atomic string. Such motion is called "rosette motion." The classical description of a rosette motion has been given by Kumm *et al.*¹⁵ While a quantum-mechanical treatment was developed by Komaki and Fujimoto,¹⁶ and Tamura and Ohtsuki.¹⁷

As was already discussed in the preceding section, axial channeling in high- Z materials can be described within

TABLE II. Number of levels and critical angles for electron axial channeling.

Target	Energy (MeV)	γ	Direction	Critical angle ψ_c	Number of levels n_a
Mo	4	8.8	$\langle 100 \rangle$	0.75	20.6
	5	10.7	$\langle 100 \rangle$	0.68	25.1
Mo	4	8.8	$\langle 110 \rangle$	0.63	14.5
	5	10.7	$\langle 110 \rangle$	0.57	17.8
Mo	4	8.8	$\langle 111 \rangle$	0.81	23.8
	5	10.7	$\langle 111 \rangle$	0.73	29.0
W	4	8.8	$\langle 111 \rangle$	1.07	28.6
	5	10.7	$\langle 111 \rangle$	0.97	35.0

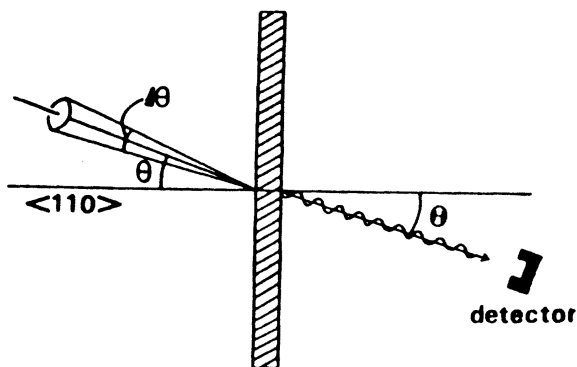


FIG. 1. Geometry of channeling radiation.

the framework of classical mechanics. But certain physical effects connected with channeling can only be explained in terms of quantum theory.

IV. NUMERICAL RESULTS AND DISCUSSIONS

Using the classical collision approximation and classical electrodynamics, we have calculated the channeling radiation emitted by low-energy electrons going through a crystal of high- Z materials along major axes. In the present simulation, 5-MeV electrons are impinged on a thin single crystal of Mo and W (see Fig. 1). The angular divergence $\Delta\theta$ of the electron beam was taken into account. As is seen in Table II, the number of quantum states for 5-MeV electrons in crystals of high- Z materials such as Mo and W is larger than twenty, and so a classical approach is reasonable.

A. Axial dependence of channeling radiation

Radiation intensities are calculated, for 5-MeV electrons impinging on the (100), (110), and (111) faces of a 1- μm -thick Mo single crystal. The angular divergence is taken as 0.5°, and temperature is set equal to 300 K. The

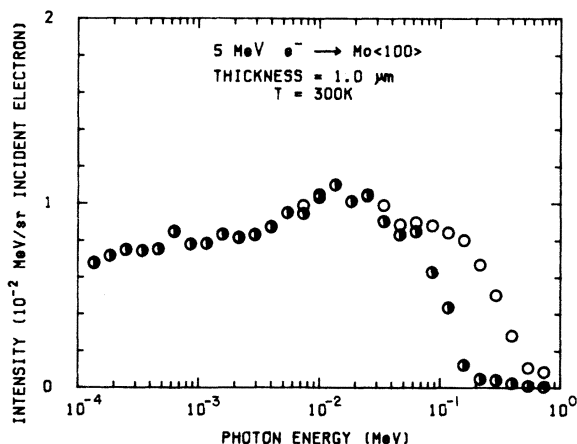


FIG. 2. Photon spectra in the forward direction for 5-MeV electrons in the $\langle 100 \rangle$ axis of a 1- μm -thick Mo crystal. The angular divergence of the electron beam is 0.5° and the temperature is 300 K.

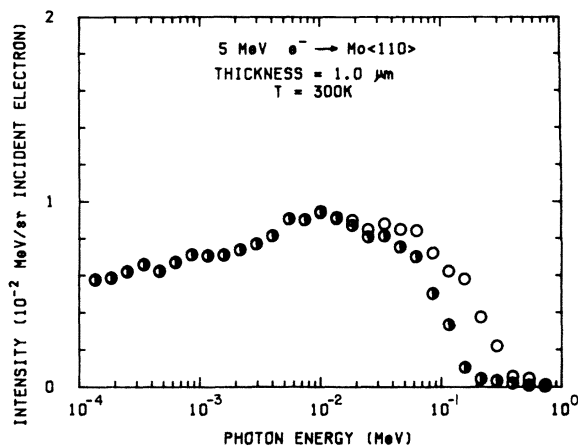


FIG. 3. Photon spectra in the forward direction for 5-MeV electrons in the $\langle 110 \rangle$ axis of a 1- μm -thick Mo crystal. The angular divergence of the electron beam is 0.5° and the temperature is 300 K.

numerical results for the $\langle 100 \rangle$, $\langle 110 \rangle$, and $\langle 111 \rangle$ axes are shown in Figs. 2, 3, and 4, respectively. The photon spectra with \bullet marks are calculated using rough mesh intervals for the Fourier-transform integral in Eq. (4). The upper bound-photon energy $\hbar\omega_{\text{max}}$ of axial-channeling radiation can be roughly estimated as $\omega_{\text{max}} = 2\gamma\psi_c/r_c$, where r_c is the critical distance above which the electron will not undergo dechanneling. Since r_c is roughly equal to the screening length a , using this a yields $\hbar\omega_{\text{max}}$ of 185, 155, and 200 keV for $\langle 100 \rangle$, $\langle 110 \rangle$, and $\langle 111 \rangle$, respectively. This is the reason why photon spectra with \bullet marks, which do not include the high-frequency component, decrease rapidly near $\hbar\omega = 100$ keV.

The profiles of emitted photon spectra show large low-energy enhancements and resemble the photon spectrum observed by Swent *et al.*⁴ for 56-keV electrons in the $\langle 110 \rangle$ channel of a 18- μm -thick silicon crystal. The maximal photon energies of the calculated spectra are listed in Table III where the photon number per angstrom, per unit solid angle, and per ampere are also listed for each case.

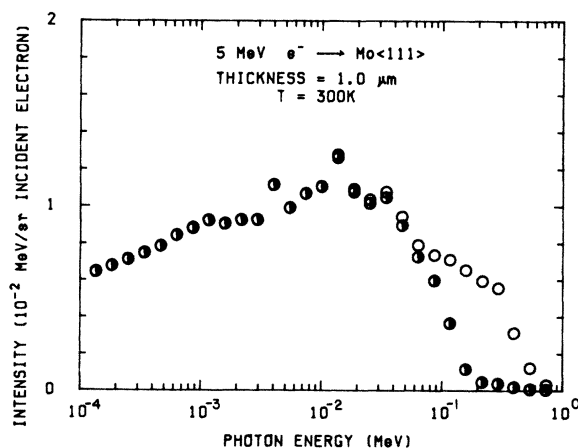


FIG. 4. Photon spectra in the forward direction for 5-MeV electrons in the $\langle 111 \rangle$ axis of a 1- μm -thick Mo crystal. The angular divergence of the electron beam is 0.5° and the temperature is 300 K.

TABLE III. Maximal photon energies and emitted photon numbers at the maximal photon energy for electron channeling along various axes.

Target	Energy (MeV)	Direction	$\Delta\theta$	Temperature	Thickness (μm)	Maximal photon energy (keV)	Photon numbers ^a $10^{17}/\text{\AA} \text{ A sr sec}$
Mo	5	$\langle 100 \rangle$	0.5°	300	1.0	14	0.78
Mo	5	$\langle 110 \rangle$	0.5°	300	1.0	10	0.47
Mo	5	$\langle 111 \rangle$	0.5°	300	1.0	16	0.90
Mo	5	$\langle 111 \rangle$	0.5°	10	1.0	30	2.33
W	5	$\langle 111 \rangle$	0.5°	300	1.0	25	3.84
Mo	5	$\langle 111 \rangle$	0.5°	300	0.25	12	0.30
Mo	5	$\langle 111 \rangle$	0.5°	300	0.50	14	0.55
Mo	5	$\langle 111 \rangle$	0.5°	300	0.75	14	0.67
Mo	5	$\langle 111 \rangle$	0.5°	300	1.0	16	0.90
Mo	5	$\langle 111 \rangle$	0.5°	300	1.5	18	1.2
Mo	5	$\langle 111 \rangle$	0.5°	300	2.0	23	1.4

^aPhoton numbers at the maximal photon energy.

One interesting point is the relatively flat feature of the $\langle 110 \rangle$ spectrum. This is due to the fact that the beam angular spread of $\Delta\theta=0.5^\circ$ is comparable to the critical angle for $\langle 110 \rangle$ axial channeling (see Table II).

According to Kumakhov's classical estimate for the axial-channeling radiation of a relativistic electron, the total intensity is given by

$$I = \frac{3}{2} \frac{Z^2 e^6}{c^3} \frac{\gamma^3}{m (r^2)^2}, \quad (8)$$

where $\overline{r^2}$ is the mean-square radius of the spiral about the string. For the present cases, we have the following inequalities:

$$(\overline{r^2})_{\langle 111 \rangle} < (\overline{r^2})_{\langle 100 \rangle} < (\overline{r^2})_{\langle 110 \rangle}.$$

This explains why we get the most intensive radiation for the $\langle 111 \rangle$ axial channeling as is shown in Table II and Figs. 2, 3, and 4.

In order to investigate the large enhancement in the higher-energy region ($\hbar\omega > 100$ keV), we have calculated the photon spectrum for $\theta=3.0^\circ$ relative to the $\langle 100 \rangle$ axis but leaving the detector set to face the direction of the incident electron beam. The result is shown in Fig. 5. In this case, the maximal photon energy is 86 keV, which is larger than the expected photon energy radiated by channeling electrons. One possibility is the contribution of coherent bremsstrahlung. As is well known, coherent bremsstrahlung is an interference effect caused by the lattice periodicity and its photon spectrum will have peaks at

$$n = 4\pi\gamma^2 \frac{c\theta}{d_p},$$

where $n=1,2,3,\dots$ ¹⁸ For 5-MeV electrons intersecting the (100) plane at an angle of 3° , the characteristic photon energy is 83 keV. This is in good agreement with the maximal energy in the photon spectrum of Fig. 5. Enhancement in the higher region of Figs. 2, 3, and 4 may be mainly due to the coherent bremsstrahlung of dechanneled electrons.

B. Temperature and thickness dependence of channeling radiation

At finite temperature, the atoms in the string are thermally deviated from their equilibrium positions and corresponding changes in the transverse Hamiltonian alter the character of the tightly bound states. Thermal vibration is responsible for the finite depth of the ground states and increases with rising temperature. This aspect is clearly shown in Fig. 6, where the photon spectra Mo $\langle 111 \rangle$ at 10 and 300 K are plotted versus the photon energy.

Thickness dependence of the photon intensity is illustrated in Fig. 7 for 5-MeV electrons in the $\langle 111 \rangle$ channel. For this range of thickness, the intensity radiated by channeling electrons shows a nearly linear proportionality to the thickness of crystal, since the dechanneling length is

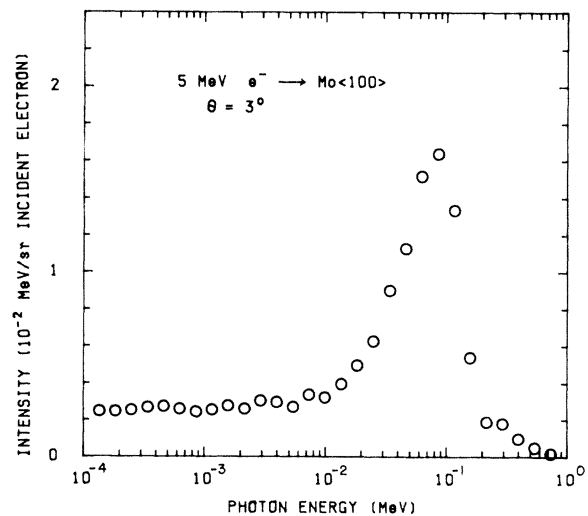


FIG. 5. Photon spectrum in the forward direction for 5-MeV electrons directed at the (100) face with an angle of 3° relative to the $\langle 100 \rangle$ axis of $1\text{-}\mu\text{m}$ -thick Mo crystal. The angular spread of the electron beam is 0.5° .

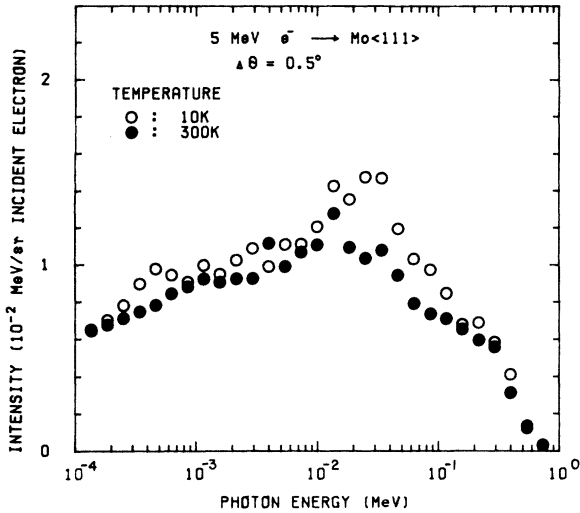


FIG. 6. Temperature dependence of photon spectra in the forward direction for 5-MeV electrons in the $\langle 111 \rangle$ axis of 1- μm -thick Mo crystal. The beam angular divergence is 0.5° .

much larger than 2.0×10^{-4} cm.¹⁸ It is interesting that the maximal photon energies becomes slightly larger as the thickness increases.

C. Incident-angle dependence of channeling radiation

The incident angle determines the initial population of the various levels. Therefore, in this section, the channeling radiation will be calculated under the condition of $\Delta\theta = 0^\circ$, since the entrance condition at the surface is more

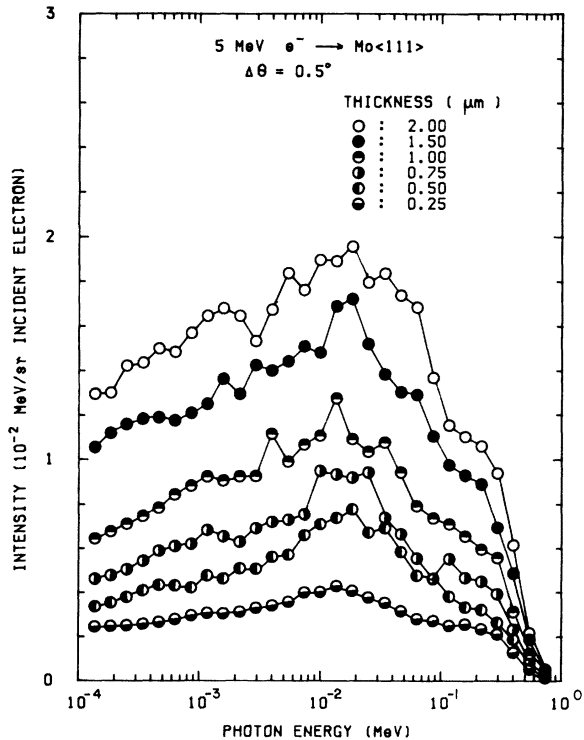


FIG. 7. Thickness dependence of photon spectra for 5-MeV electrons in the $\langle 111 \rangle$ axis of Mo crystal. The temperature is 300 K and the beam angular divergence is 0.5° .

clearly specified than the case of finite angular spread.

Figure 8 shows the incident-angle dependence of the channeling radiation, where the angles 0.0° , 0.4° , and 0.8° are relative to the $\langle 111 \rangle$ axis and the detector is set at the direction of the incident electron beam. The maximal photon energy of each angle of incidence is seen to increase slightly with increasing the angle of incidence (see Table III), and the profiles of the photon spectra of $\theta = 0^\circ$, 0.4° , and 0.8° resemble each other. At the higher photon energies the channeling radiation of $\theta = 0.4^\circ$ is most intensive. This may be due to the fact that the angle $\theta = 0.4^\circ$ is nearly equal to half of the critical angle of a 5-MeV electron.

D. Channeling radiation and ordinary bremsstrahlung in high-Z material

Channeling-radiation intensity begins to exceed that of ordinary bremsstrahlung at an electron energy of several MeV. Ordinary bremsstrahlung is caused by multiple scattering of electrons on atoms and electrons in solids and thus has a very broad angular distribution. Channeling radiation, on the other hand, is highly forward directed and may provide a powerful flux of x-ray or γ -ray quanta. The photon intensity of the ordinary bremsstrahlung is given by

$$\frac{d^2E}{d\hbar\omega d\Omega} = 3.8 \times 10^{-4} \gamma^2 \quad (9)$$

in the relativistic limit for the optimum thickness L_{opt} , where

$$L_{\text{opt}} = 5.4 \times 10^{-4} R.$$

Here, R is the radiation length and it is roughly given by

$$R = \left[1.30 \times 10^{-4} \frac{\rho Z^2}{M} \ln \left(\frac{233}{Z^{1/3}} \right) \right]^{-1},$$

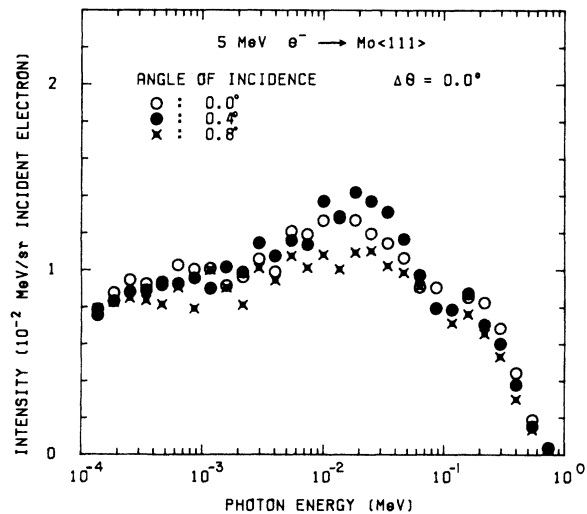


FIG. 8. Incident angle dependence of photon spectra for 5-MeV electrons. The emitted radiation is for the direction of the $\langle 111 \rangle$ axis, the temperature is 300 K, and the beam angular divergence is 0.5° .

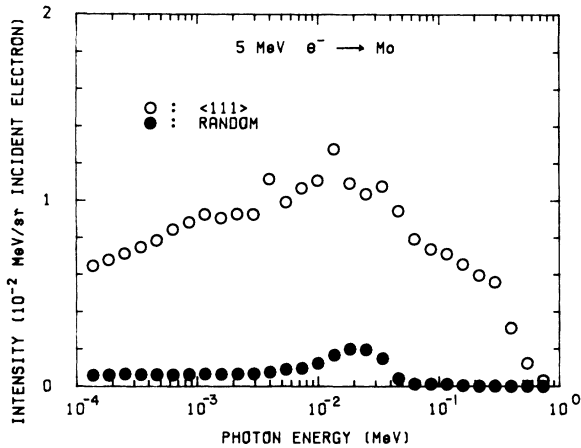


FIG. 9. Comparison of the axial-channeling radiation with the forward-directed bremsstrahlung for 5-MeV electrons in a 1- μm -thick Mo crystal. The photon emission is in the direction of an incident electron beam, the angular divergence of the beam is 0.5° , and temperature is 300 K. The incident angles are, respectively, $\theta=0^\circ$ and $\theta=9^\circ$ relative to the $\langle 111 \rangle$ axis for the forward-directed bremsstrahlung and channeling radiation.

where M is the atomic mass of the target atom, and ρ is the density of the target material.

Equation (9) tells us that the photon intensity of ordinary bremsstrahlung of 5-MeV electrons in the Mo target is comparable to that of channeling radiation. It is difficult, however, to apply Eq. (9) directly to low-energy bremsstrahlung, since the angular distribution of the emitted photon by low-energy electrons is not so forward directed.

In order to predict the photon intensity of bremsstrahlung emitted by low-energy electrons, we have calculated

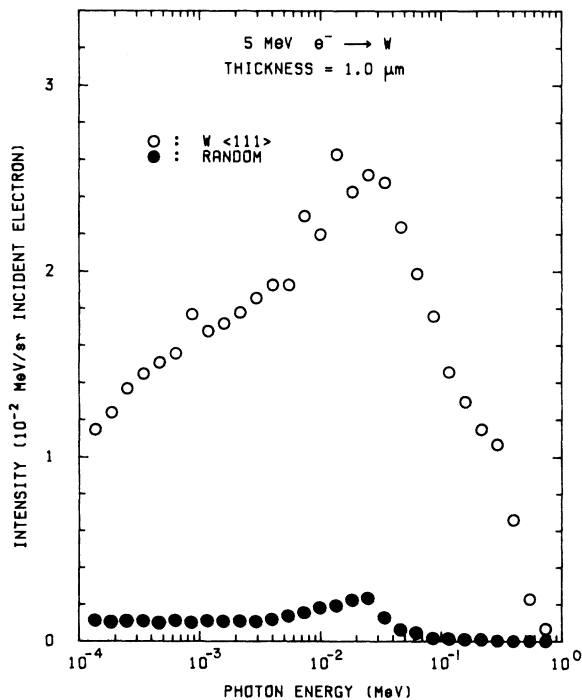


FIG. 10. The same as in Fig. 9 but for 1- μm -thick W crystal.

the forward-directed photon intensity under the condition of $\theta=9^\circ$ and $\Delta\theta=0.5^\circ$. Comparison of channeling radiation with the forward-directed radiation is shown in Fig. 9, where open circles and solid circles correspond to channeling radiation and forward-directed bremsstrahlung, respectively. The ratio of the former radiation to the latter radiation is about 10 in the photon-energy region less than 100 keV.

More intensive radiation may be expected with a higher- Z material. The case of a 1- μm -thick W crystal is shown in Fig. 10. In this case, the maximum photon intensity of channeling radiation in W $\langle 111 \rangle$ is higher than that in Mo $\langle 111 \rangle$ by a factor of about 2.2, while the ratio of the intensity of channeling radiation to that of forward-directed bremsstrahlung is about thirteen at the peak of the channeling radiation spectrum.

In Fig. 11 the photon numbers radiated per an electron, per angstrom, and per unit solid angle are plotted against the wavelength for 5-MeV electrons directed along the $\langle 111 \rangle$ axis of 1- μm -thick Mo and W crystals under the same conditions. Note that the photon number as a function of wavelength is peaked at a wavelength corresponding to a photon energy larger than the maximal photon energy. The values of maximum photon number per angstrom are 0.28 and 0.13 for W $\langle 111 \rangle$ and Mo $\langle 111 \rangle$, respectively.

We may compare the channeling-radiation intensity with the x-ray intensity from an ordinary x-ray tube RU-1500 which is 4.3×10^{15} photons/ \AA A s sr for 50 keV electrons on a W target at 20 keV photon energy. From Table III, the corresponding value for 5-MeV electrons along W $\langle 111 \rangle$ is 3.84×10^{17} photons/ \AA A s sr. Channeling radiation is clearly more intense than any x-ray tube source.

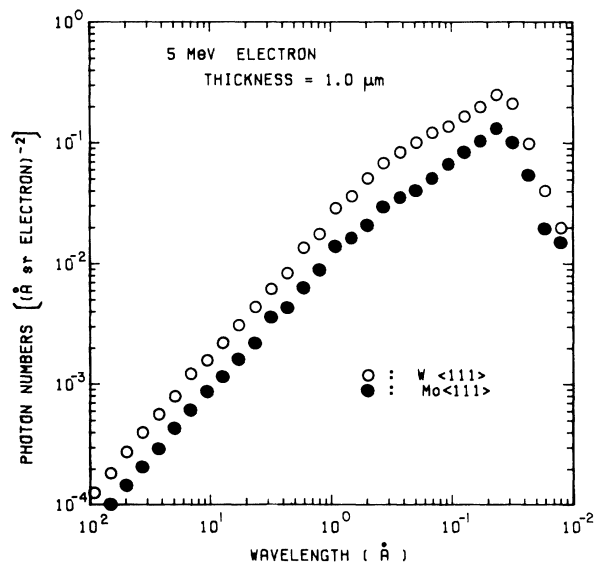


FIG. 11. Photon numbers per an electron, per angstrom, and per unit solid angle are plotted against the wavelength of the radiated photon. The angular divergence of the 5-MeV electron beam is 0.5° , the temperature is 300 K, and the thickness of Mo and W crystal is 1 μm .

V. CONCLUSION

With the use of the classical binary-collision approximation and classical electrodynamics, channeling radiation emitted by axially-channeled 5-MeV electrons in high-Z materials, such as Mo and W, has been studied. Axial dependence of the channeling radiation was investigated for the three major axes of a Mo single crystal, i.e., $\langle 100 \rangle$, $\langle 110 \rangle$, and $\langle 111 \rangle$. The calculated maximal photon energy and the intensity of the photon spectrum depend strongly on the string potential (mainly the distance between the atoms in the string).

Thermal vibration is seen to have an effect on the axial channeling of electrons. This is reflected by the reduced photon intensity as well as the maximal photon energy.

The thickness of the crystal affects the maximal photon energy as well as the intensity radiated by channeling electrons. When the thickness is less than the dechanneling length, the intensity shows a near proportionality to the thickness of material.

The angular variation of the photon intensities reflects the variation of population of initial states. For $\theta=0^\circ$, the

photon intensities in the low-energy region is relatively large. However, the most intense radiation will be observed for an angle of incidence less than the critical angle because more states are populated.

Comparison of the intensity of the channeling radiation with that of the forward-directed bremsstrahlung was undertaken. For 5-MeV electrons, the ratio of the former intensity to the latter intensity in the direction of the incident electron beam is about ten on average. This large ratio is reasonable since the angular spread of ordinary bremsstrahlung is inversely proportional to the half-power of the radiation length.¹⁴

A large ratio of the channeling radiation intensity to the intensity from an intense x-ray tube was also obtained. This suggests a new x-ray source for the ordinary x-ray laboratory.

ACKNOWLEDGMENT

These authors would like to express their gratitude to Mr. K. Horihata for his assistance in numerical calculations.

-
- ¹A. A. Vorobiev, V. V. Kaplin, and S. A. Vorobiev, *Nucl. Instrum. Methods* **127**, 265 (1975).
²M. A. Kumakhov, *Phys. Lett.* **57A**, 17 (1976).
³M. J. Alguard, R. L. Swent, R. H. Pantell, B. L. Berman, S. D. Bloom, and S. Datz, *Phys. Rev. Lett.* **30**, 265 (1979).
⁴R. L. Swent, R. H. Pantell, M. J. Alguard, B. L. Berman, S. D. Bloom, and S. Datz, *Phys. Rev. Lett.* **43**, 1723 (1979).
⁵B. N. Kalinin, V. V. Kaplin, A. P. Potalitin, and S. A. Vorobiev, *Phys. Lett.* **70A**, 447 (1979).
⁶J. U. Andersen and E. Laesgaard, *Phys. Rev. Lett.* **44**, 1079 (1980).
⁷J. U. Andersen, E. Bonderup, E. Laesgaard, B. B. Marsh, and A. H. Sorensen, *Nucl. Instrum. Methods* **194**, 209 (1982).
⁸K. Komaki, F. Fujimoto, and A. Ootsuka, *Nucl. Instrum. Methods* **194**, 243 (1982).
⁹M. A. Kumakhov, *Zh. Eksp. Teor. Fiz.* **72**, 1489 (1977) [*Sov. Phys.—JETP* **45**, 781 (1977)].
¹⁰M. T. Robinson and I. M. Torrens, *Phys. Rev. B* **9**, 1008 (1974).
¹¹J. D. Jackson, *Classical Electrodynamics* (Wiley, New York, 1975).
¹²Y. Yamamura and Y. H. Ohtsuki, *Phys. Rev. B* **24**, 3430 (1981).
¹³L. T. Chadderton, in *Channeling*, edited by D. V. Morgon (Wiley, London, 1973), p. 287.
¹⁴J. Lindhard, K. Dans. *Vidensk. Selsk. Mat. Fys. Medd.* **34**, No. 14 (1965).
¹⁵H. Kumm, F. Bell, R. Sitzmann, H. J. Kreiner, and D. Harder, *Radiat. Eff.* **12**, 53 (1972).
¹⁶K. Komaki and F. Fujimoto, *Phys. Lett.* **49A**, 445 (1974).
¹⁷A. Tamura and Y. H. Ohtsui, *Phys. Status Solidi B* **62**, 477 (1974).
¹⁸R. Wedell, *Phys. Status Solidi B* **99**, 11 (1980).